Direct Neutron Capture for Magic–Shell Nuclei

E. Krausmann, W. Balogh, H. Oberhummer
Institut für Kernphysik, Technische Universität Wien, Wiedner Hauptstrasse 8–10, 1040 Vienna, Austria

T. Rauscher
Institut für Kernchemie, Universität Mainz, Fritz-Strassmann–Weg 2, 55099 Mainz, Germany
and
Institut für theoretische Physik, Universität Basel, Klingelbergstr. 82, 4056 Basel, Switzerland

K.-L. Kratz, W. Ziegert
Institut für Kernchemie, Universität Mainz, Fritz-Strassmann–Weg 2, 55099 Mainz, Germany

In neutron capture for magic–shell nuclei the direct reaction mechanism can be important and may even dominate. As an example we investigated the reaction ^{48}Ca(n,γ)^{49}Ca for projectile energies below 250 keV in a direct capture model using the folding procedure for optical and bound state potentials. The obtained theoretical cross sections are in agreement with the experimental data showing the dominance of the direct reaction mechanism in this case. The above method was also used to calculate the cross section for ^{50}Ca(n,γ)^{51}Ca.

24.50.+g, 25.40.Lw, 97.10.Cv

I. INTRODUCTION

Attempts to understand low- and medium–density ($n_{\rm n} \leq 6 \cdot 10^{16}$ n/cm^3) neutron–capture nucleosynthesis processes require temperature–dependent Maxwellian–averaged capture cross sections. For radioactive isotopes, where these cross sections cannot be measured they are usually calculated within global Hauser–Feshbach models. Whereas this statistical approach appears to be applicable for nuclides in between neutron shells exhibiting sufficiently high level densities, it certainly will fail for neutron–magic isotopes with only a few widely spaced resonances. For such cases apart from compound–nucleus (CN) capture, direct (DI) reaction processes are important.

As an example we investigated the reaction ^{48}Ca(n,γ)^{49}Ca to test our method, where, in principle, all necessary information is already available from various experiments [1–9]. We also calculated the reaction ^{50}Ca(n,γ)^{51}Ca, which may be of importance in connection with an interpretation of the ^{50}Ti overabundance observed in FUN inclusions of the Allende meteorite (see e.g. [10,11]).

In the CN mechanism the projectile merges with the target nucleus and excites many degrees of freedom of the CN. The excitation proceeds via a multistep process and has a reaction time typically of the order 10^{-14} s to 10^{-20} s. After this time the CN decays into various exit channels. In the DI process the projectile excites only a few degrees of freedom (e.g. single–particle or collective). The excitation proceeds in one single step and has a characteristic time scale of 10^{-21} s to 10^{-22} s. This corresponds to the time it takes the projectile to pass through the target nucleus; this time is much shorter than the reaction time of the CN processes.

For thermonuclear (in the keV region) and thermal (in the meV region) projectile energies the competition between the different reaction mechanisms is quite complicated. Normally the CN formation prevails below projectile energies of approximately 10 to 20 MeV. However, for light nuclei and magic nuclei the CN formation is often suppressed because there are no CN levels that can be populated. In this case the DI reaction mechanism can dominate the nuclear reaction.

II. NUCLEAR–STRUCTURE INFORMATION

The nuclear structure of the compound nucleus ^{49}Ca is of special interest because of the expected simple single–particle character of the low–lying states formed by coupling 2p$_{3/2}$, 1f$_{5/2}$ and 2p$_{1/2}$ neutrons to the $J^\pi = 0^+$ ground state of ^{48}Ca. At higher excitation energies many bound levels can be described by 2particle–1hole configurations [3]. Information on neutron–unbound states in ^{49}Ca ($S_{\rm n} = 5.142$ MeV) comes from three different experimental sources: neutron–capture and transmission measurements [2,6–8], (d,p)–reaction work [3,9], and high–resolution spectroscopy of β–delayed neutron (βdn) decay [4,5] of $J^\pi = 3/2^+$ in ^{49}K. As is discussed in Ref. [12], the ^{49}K(β^-)^{49}Ca(n)^{48}Ca decay can be considered as inverse process to s– and d–wave neutron capture on ^{48}Ca. Companion theoretical studies to Ref. [2] by Divadeenam et al. [13] (2p–1h doorway model), to Refs. [4,5] by Dobado and Poves [14] (complete sd–fp shell model), as well as own QRPA shell–model calculations (Gamow–Teller strength), using the code of Möller and Randrup [15] agree quite well with the experimental observations. The most remarkable result is the absence of $J^\pi = 1/2^+$ states (s–wave resonances) up to at least $S_\mathrm{n} + 800\,\mathrm{keV}$, which can be understood in terms of the specific quasiparticle structure of ^{49}Ca. The second observation is that the d–wave strength is considerably larger than the p–wave strength. This is due to the existence of a d–wave giant resonance for $A = 48$. Finally, no strong neutron–resonances were identified below 158 keV. The two very small resonances at 20 keV and 107 keV only found in neutron capture [7], but not in β–delayed neutron decay [4,5] and not in the (d,p)–reaction [3,9], are probably also d–wave resonances with $\Gamma_\mathrm{n} < \Gamma_\gamma$.

With this nuclear–structure information on ^{49}Ca average continuum (HF) and resonance (Breit–Wigner, BW) neutron–capture rates were derived using the code SMOKER [12,16]. When comparing these values with the measured 30 keV Mawellian–averaged capture cross section of ^{48}Ca (See Refs. [6,7]), one can draw the following conclusions: The statistical–model (HF) prediction agrees with the measured cross section at 30 keV of about 1 mb; this result must, however, be regarded as completely fortuitous. The contribution of the resonances, i.e. the BW cross section, is only about 5% of the total neutron–capture rate. Hence, in the case of the doubly–magic nucleus ^{48}Ca, 95% must be due to direct reaction processes.

In contrast to ^{48}Ca(n,γ), the nuclear structure information on the radioactive target ^{50}Ca and the compound nucleus ^{51}Ca are scarce. Some bound levels without spin assignment are known from reaction work and ^{51}K β–decay [17], and the singles spectrum of βdn's has been measured (see Fig. 1, taken from Ref. [4]; the continuum underlying the peaks in the spectrum is due to the response of the spectrometer used). Due to Gamow-Teller selection rules, the peaks seen in the spectrum correspond to $J^\pi = 1/2^+$ and $3/2^+$ neutron–unbound states in ^{51}Ca. According to the inverse relationship between βdn–decay and neutron capture [4], these states represent s– and d–wave resonances in ^{50}Ca(n,γ)^{51}Ca. Similar to the compound nucleus ^{49}Ca, the most remarkable result is the absence of $J^\pi = 1/2^+$ states up to 0.85 MeV beyond the neutron separation energy ($S_\mathrm{n} = 4.4\,\mathrm{MeV}$ [18]). This results in a resonance capture cross section of $\langle\sigma^\mathrm{CN}\rangle \simeq 8.5\cdot 10^{-15}$ mb when using the BW–formalism of the SMOKER code [12,16]. If this were the total capture rate for ^{50}Ca, in any astrophysical s– and nβ–type neutron–capture process [6,10] the build–up of $A > 50$ Ca isotopes would be strongly hindered by successful competition of β–decay. With this, a strong overabundance of ^{50}Ti — as observed in certain meteoritic inclusions (for discussion see Refs. [10,11]) — would result.

However, also in the case of ^{50}Ca neutron capture, it is not unlikely that $\langle\sigma^\mathrm{CN}\rangle$ represents only a small fraction of the total cross section which may be dominated by the DI reaction rate. Shell–model considerations (using the QRPA code of Möller et al. [15,19]) support this possibility. When assuming the compound nucleus ^{51}Ca to be spherical, its ground state has the $\nu\mathrm{p}_{3/2}$ configuration ($J^\pi = 3/2^-$). The two lowest excited levels are predicted to be the $\nu\mathrm{p}_{1/2}$ and $\nu\mathrm{f}_{5/2}$ shell–model states at about 1.177 MeV and 1.209 MeV, respectively. From the 0^+ ground state of ^{50}Ca indeed strong p–wave radiative capture can be expected to the $J^\pi = 3/2^-$ and $1/2^-$ levels in ^{51}Ca. Another interesting result of our QRPA calculations is the prediction of the lowest–energy $J^\pi = 1/2^+$ and $3/2^+$ states of $\nu\mathrm{g}_{9/2}$ shell–model origin around 5.50 MeV in ^{51}Ca. This is in good agreement with our experimental result from the ^{51}K βdn–spectrum (Fig. 1). After correction for recoil, we obtain for the two lowest neutron–unbound $J^\pi = 1/2^+$, $3/2^+$ states $E_1^* = (S_\mathrm{n} + E_\mathrm{n1}) \simeq 5.31\,\mathrm{MeV}$ and $E_2^* = (S_\mathrm{n} + E_\mathrm{n2}) \simeq 5.37\,\mathrm{MeV}$. The neutron peaks at 1.18 MeV, 1.46 MeV, 2.20 MeV and 2.48 MeV identified in our βdn–spectrum correspond to transitions to the 2_1^+–state in ^{50}Ca and, hence, are not important for the present resonance neutron–capture considerations.

In the following, we will present our direct neutron–capture calculations using as input parameters the experimental and theoretical information given above.

III. DI-CALCULATIONS

Potential models have often been used to describe direct reactions at thermonuclear and thermal projectile energies (Ref. [20] and references therein). They are based on the description of the dynamics of the reaction by a Schrödinger equation with optical potentials in the entrance and exit channel. Such models are the Distorted Wave Born Approximation (DWBA) for transfer reactions or the Direct Capture Model (DC) for radiative capture.

The DC cross section ist given by [21]

$$\begin{aligned}\sigma^\mathrm{DC} &= \int \mathrm{d}\Omega\, \frac{\mathrm{d}\sigma^\mathrm{DC}}{\mathrm{d}\Omega_\gamma} \\ &= \int \mathrm{d}\Omega\, 2 \left(\frac{e^2}{\hbar\,\mathrm{c}}\right) \left(\frac{\mu \mathrm{c}^2}{\hbar\,\mathrm{c}}\right) \left(\frac{\mathrm{k}_\gamma}{\mathrm{k}_a}\right)^3 \frac{1}{2\,I_A + 1}\, \frac{1}{2\,S_a+1} \sum_{M_A\, M_a\, M_B,\,\sigma} |\, T_{M_A\, M_a\, M_B,\,\sigma}\,|^2\,. \qquad (1)\end{aligned}$$

The quantities I_A, I_B and S_A (M_A, M_B and M_a) are the spins (magnetic quantum numbers) of the target nucleus A, residual nucleus B and projectile a, respectively. The reduced mass in the entrance channel is given by μ. The polarisation σ of the electromagnetic radiation can be ± 1. The wave number in the entrance channel and for the emitted radiation is given by k_a and k_γ, respectively.

The multipole expansion of the transition matrices $T_{M_A\, M_a\, M_B,\,\sigma}$ including electric dipole (E1) and quadrupole (E2) transitions as well as magnetic dipole (M1) transitions is given by

$$T_{M_A\, M_a\, M_B,\,\sigma} = T^{\rm E1}_{M_A\, M_a\, M_B,\,\sigma}\, d^1_{\delta\,\sigma}(\theta) + T^{\rm E2}_{M_A\, M_a\, M_B,\,\sigma} d^2_{\delta\,\sigma}(\theta) + T^{\rm M1}_{M_A\, M_a\, M_B,\,\sigma} d^1_{\delta\,\sigma}(\theta). \tag{2}$$

The rotation matrices depend on the angle between $\vec{k}_a$ and $\vec{k}_\gamma$ which is denoted by ϑ, where $\delta = M_A + M_a - M_B$.

Defining

$$C({\rm E1}) = i\,\mu\left(\frac{Z_a}{m_a} - \frac{Z_A}{m_A}\right), C({\rm E2}) = \frac{{\rm k}_\gamma}{\sqrt{12}}\,\mu^2\left(\frac{Z_a}{m_a^2} + \frac{Z_A}{m_A^2}\right), \tag{3}$$

we can write for the transition matrices for the electric dipole (E$\mathcal{L}$ = E1) or quadrupole (E$\mathcal{L}$ = E2) transition

$$\begin{aligned} T^{\rm E\mathcal{L}}_{M_A\, M_a\, M_B,\,\sigma} = \sum_{l_a\, j_a} & i^{l_a} \langle l_a\, 0\, S_a\, M_a \mid j_a\, M_a\rangle \langle j_b\, M_B - M_A\, I_A\, M_A \mid I_B\, M_B\rangle \\ & \times \langle \mathcal{L}\,\delta\, j_b\, M_B - M_A \mid j_a\, M_a\rangle C(E\mathcal{L})\,\hat{l}_a\,\hat{l}_b\,\hat{j}_b \\ & \times \langle l_b\, 0\, \mathcal{L}\, 0 \mid l_a\, 0\rangle W(\mathcal{L}\, l_b\, j_a\, S_a; l_a\, j_b) I^{E\mathcal{L}}_{l_b\, j_b\, I_B; l_a\, j_a}. \end{aligned} \tag{4}$$

In the above expressions Z_a, Z_A and m_a, m_A are the charge and mass numbers of the projectile a and target nucleus A, respectively. The quantum numbers for the channel spin in the entrance channel and for the transferred angular momentum are denoted by j_a and j_b, respectively. Here and in the following the abbreviation $\hat{l}$ stands for $\sqrt{2l+1}$ (the same applies to other quantum numbers).

For magnetic dipole transitions we obtain

$$\begin{aligned} T^{\rm M1}_{M_A\, M_a\, M_B,\,\sigma} = \sum_{l_a\, j_a} i^{l_a}\,\sigma \Bigg[& \langle l_a\, 0\, S_a\, M_a \mid j_a\, M_a\rangle \langle j_b\, M_B - M_A\, I_A\, M_A \mid I_B\, M_B\rangle \\ & \times \langle 1\,\delta\, j_b\, M_B - M_A \mid j_a\, M_a\rangle \\ & \times \Bigg\{ \mu\left(\frac{Z_A}{m_A^2} + \frac{Z_a}{m_a^2}\right)\hat{l}_b\,\hat{j}_b\,\sqrt{l_a\,(l_a+1)} W(1\, l_a\, j_a\, S_a; l_a\, j_b) \\ & + 2\mu_a\,(-1)^{j_b - j_a}\,\hat{S}_a\,\hat{j}_b\,\sqrt{S_a\,(S_a+1)} W(1\, S_a\, j_a\, l_a; S_a\, j_b) \Bigg\} \\ & - \langle l_a\, 0\, S_a\, M_a \mid j_a\, M_a\rangle \langle j_a\, M_a\, I_A\, M_B - M_a \mid I_B\, M_B\rangle \\ & \times \langle I_A\, M_B - M_a\, 1\,\delta \mid I_A\, M_A\rangle \\ & \times\ \mu_A\,\delta_{j_a\, j_b}\sqrt{\frac{I_A+1}{I_A}}\,\Bigg] \left[\frac{\hbar\,{\rm c}}{2\, m_{\rm p}\,{\rm c}^2}\right] \delta_{l_a\, l_b}\,\hat{l}_a\, I^{M1}_{l_b\, j_b\, I_B; l_a\, j_a}, \end{aligned} \tag{5}$$

where W is the Racah coefficient, the μ_i are the magnetic moments and $m_{\rm p}$ is the mass of the proton.

The overlap integrals in Eqs. (4,5) are given by [22]

$$I^{\rm E\mathcal{L}}_{l_b\, j_b\, I_B; l_a\, j_a} = \int {\rm d}r\, U_{l_b\, j_b\, I_B}(r) \mathcal{O}^{\rm E\mathcal{L}}(r)\,\chi_{l_a\, j_a}(r) \tag{6}$$

for the electric dipole (E$\mathcal{L}$ = E1) or quadrupole (E$\mathcal{L}$ = E2) transition, and by

$$I^{\rm M1}_{l_b\,j_b\,I_B;l_a\,j_a} = \int {\rm d}r\, U_{l_b\,j_b\,I_B}(r) \mathcal{O}^{\rm m1}(r)\, \chi_{l_a\,j_a}(r) \tag{7}$$

for the magnetic dipole transition ($\mathrm{M}\mathcal{L} = \mathrm{M1}$). The radial part of the bound state wave function in the exit channel and the scattering wave function in the entrance channel is given by $U_{l_b\,j_b\,I_B}(r)$ and $\chi_{l_a\,j_a}(r)$, respectively. The radial parts of the electromagnetic multipole operators are

$$\mathcal{O}^{\rm M1}(r) = \frac{1}{2\rho}\, [\sin\rho + \rho\,\cos\rho]\,, \tag{8}$$

$$\mathcal{O}^{\rm E1}(r) = \frac{3}{\rho^3}\, \left[(\rho^2-2)\,\sin\rho + 2\,\rho\,\cos\rho\right] r, \tag{9}$$

$$\mathcal{O}^{\rm E2}(r) = \frac{15}{\rho^5}\, \left[(5\,\rho^5-12)\,\sin\rho + (12-\rho^2)\,\rho\,\cos\rho\right] r^2. \tag{10}$$

In the long wavelength approximation — applicable in our case, since $\rho = k_\gamma r \ll 1$ — these quantities reduce to

$$\mathcal{O}^{\rm M1}(r) \simeq 1, \tag{11}$$

$$\mathcal{O}^{\rm E1}(r) \simeq r, \tag{12}$$

$$\mathcal{O}^{\rm E2}(r) \simeq r^2. \tag{13}$$

The most important ingredients in the potential models are the wave functions for the scattering and bound states in the entrance and exit channels. In calculations performed by our group the potentials are determined by using the folding procedure [20]. In this approach the number of open parameters is reduced considerably compared to more phenomenological potentials (e.g. Saxon–Woods potentials). The nuclear densities are derived from nuclear charge distributions [23] and folded with an energy and density dependent nucleon–nucleon (NN) interaction $v_{\rm eff}$ [24]:

$$V(R) = \lambda\, V_{\rm F}(R) = \lambda \int\!\!\int \rho_a(\vec{r}_1)\rho_A(\vec{r}_2)\, v_{\rm eff}\,(E,\rho_a,\rho_A,s)\, {\rm d}\vec{r}_1{\rm d}\vec{r}_2. \tag{14}$$

The variable s in the NN interaction term is given by

$$s = |\vec{R} + \vec{r}_2 - \vec{r}_1| \tag{15}$$

with $\vec{R}$ being the separation of the centers of mass of the two colliding nuclei. The normalization factor λ accounts empirically for Pauli repulsion effects and dispersive parts in the potential $V(R)$ that are not included in the folding potential $V_{\rm F}(R)$. This parameter can be adjusted to elastic scattering data and/or bound and resonant state energies of nuclear cluster states and at the same time ensures the correct behaviour of the wave functions in the nuclear exterior.

For the calculation of the DI capture cross section (Eqs. (1–14)) we used the code TEDCA [25]. The folding potentials (Eq. (14)) were determined with the help of the code VOLD [26].

The reaction ^{48}Ca(n,γ)^{49}Ca was calculated for projectile energies below 250 keV. For the potential ^{48}Ca + n in the entrance and exit channel we used

$$V(R) = \lambda\, V_{\rm F}(R) \tag{16}$$

where $V_{\rm F}$ is the folding potential of Eq. (14). The strength of the potential $\lambda_{\rm i}$ in the entrance channel was determined using neutron scattering data obtained from [8]. The data was fitted to pure s-wave scattering with $\sigma = 0.019$ b resulting in a $\lambda_{\rm i}$ of 0.93357 and giving a volume integral of 436.9 MeV fm^3.

For the optical potential in the entrance channel we neglected the imaginary part potential because the flux into the other channels is very small. One may wonder, if the capture process would not itself produce a large damping, because at low energies the capture cross section is larger than the elastic cross section. For instance, at thermal energies the neutron–capture cross section of ^{48}Ca is about 1 b, whereas the elastic neutron cross section is about 0.02 b. However, this can be explained by the different phase–space factors for the capture and elastic cross sections. For the capture cross section near threshold one can write $\sigma_{\rm c} \approx (4\pi\, R/k_a)(-{\rm Im}f_0/|f_0|^2)$, where f_0 is the logarithmic derivative at a radial distance R. The elastic cross section is about constant for projectiles near threshold, whereas the capture cross section has the well known $1/v$–behaviour. From the thermal value of the capture cross section, using $R = 4.5$ fm, $-{\rm Im}f_0/|f_0|^2 \approx 6\cdot 10^{-5}$ is obtained. Since this expression can be regarded as a measure of damping in the entrance channel, we see that the damping effects are rather small. Therefore, at low energies the large value of the capture cross section ($1/v$–behaviour) compared to the elastic cross section (only weakly energy–dependent) is

due to the phase–space factors and does not result in additional damping effects.
For the exit channels in ^{49}Ca we fitted $\lambda_{\rm f}$ to reproduce the experimental neutron separation energies in ^{49}Ca. We obtained $\lambda_{\rm f}$ = 0.9648, 0.8863, 0.8417, 1.6745, 1.6014 and 1.5885 for the $2p_{3/2}$, $2p_{1/2}$, $1f_{5/2}$, $2f_{5/2}$, $3p_{3/2}$ and $3p_{1/2}$ state in ^{49}Ca, respectively. Spins, excitation energies, Q–values and spectroscopic factors for the transitions to the ground and excited states are listed in Table I [9].

IV. RESULTS AND DISCUSSION

The theoretical cross section $\sigma^{\rm th}$ is obtained from the direct capture cross section $\sigma^{\rm DC}$ in Eq. (1) as a sum over each final state i by

$$\sigma^{\rm th} = \sum_i C_i^2 S_i \sigma_i^{\rm DC}. \tag{17}$$

In our case the isospin Clebsch-Gordan coefficients C_i are 1. The spectroscopic factors S_i describe the overlap between the antisymmetrized wave functions of ^{48}Ca + n and the final state in ^{49}Ca. We obtained the values for the spectroscopic factors given in Table I from a recent analysis of ^{48}Ca(d,p)^{49}Ca [9].

The most important contributions to the direct capture cross section are given by the transitions to the ground and first excited state in ^{49}Ca with a Q–value of 5.142 MeV and 3.121 MeV, respectively (Table II). For the transition to the ground state (g.s.) we obtained the Maxwellian–averaged direct capture cross section at 30 keV

$$\langle\sigma^{\rm th}_{\rm g.s.}\rangle = 0.791\,{\rm mb},$$

and for the transition to the first excited state at 2.021 MeV

$$\langle\sigma^{\rm th}_{\rm exc.}\rangle = 0.222\,{\rm mb}.$$

With the small contributions of the $3p_{3/2}$ state at 4.069 MeV and the $3p_{1/2}$ state at 4.261 MeV we obtain $\langle\sigma^{\rm th}_{\rm exc.}\rangle =$ 1.04 mb for the Maxwellian–averaged direct capture cross section at 30 keV. The cross section for the transitions to the other high–spin states in the final nucleus can be neglected (Table II). This is due to the fact that only for final p–states an E1–transition with s–wave neutrons in the entrance channel is possible.

Fig. 2 shows the contributions to the direct capture at a projectile energy of 30 keV as a function of the radial distance from the target nucleus given by the integrand of Eq. (6). It is interesting to note that the important contributions to the investigated capture reaction come from the nuclear surface (4.5–5 fm) as well as from the nuclear exterior.

In Table III the theoretical DC cross sections $\sigma^{\rm th}$ obtained in this work are compared to the experimental data $\sigma^{\rm exp}$. As can be seen from Table III and Fig. 3 the experimental data can be reproduced excellently for the thermal as well as for the thermonuclear energy region by our DC–calculations. In Fig. 3 the theoretical direct capture cross section (solid line) is shown together with the experimental data of Cranston and White [1], Käppeler et al. [6] and Carlton et al. [7]. In this plot we find the well known $1/v$ behaviour of the experimental as well as the theoretical cross section ranging from the meV to the MeV region.

We also calculated the direct capture cross section for the reaction ^{50}Ca(n,γ)^{51}Ca. To obtain the ^{50}Ca + n–potential we used the density distribution obtained from QRPA calculations [15]. The Q–value for the $p_{3/2}$ transition to the ground state is given by 4.4 MeV [18]. The resonant states $J^\pi = 1/2^+$ and $3/2^+$ of $\nu g_{9/2}$ shell–model origin around 5.50 MeV mentioned in the introduction are of 2p–1h type and therefore cannot be reached by direct capture. They have not been included in our calculation. The spin and the excitation energy of the first excited state is $1/2^-$ at 1.1768 MeV. The above values and the spectroscopic amplitudes were obtained from QRPA shell model calculations using a folded–Yukawa single–particle and a Lipkin–Nogami pairing model [15]. These input parameters (see Table IV) yield

$$\langle\sigma^{\rm DC}\rangle = 0.7\,{\rm mb}$$

for the Maxwellian–averaged cross section of ^{50}Ca(n,γ)^{51}Ca at 30 keV. The lower value of this cross section compared to the cross section of 1.04 mb for ^{48}Ca(n,γ)^{49}Ca is mainly due to the lower Q–value.

These results are important for astrophysical r– and α–process calculations. Previously, the rates were calculated in the statistical model which yields a vanishing cross section for ^{50}Ca(n,γ)^{51}Ca. Therefore, the turning point in the neutron–capture path was at ^{48}Ca because of the very small cross sections of the heavier isotopes. With the above considerably higher cross section (comparable to the one of ^{48}Ca(n,γ)^{49}Ca) the path can continue beyond ^{48}Ca or even beyond ^{50}Ca. Recent network calculations prove that possibility at least for low entropies of the Type II supernova hot entropy bubble [27]. This underlines the importance of direct capture in astrophysical environments.

V. SUMMARY

We used the reaction ^{48}Ca(n,γ)^{49}Ca as a test case for calculating the DC cross section, since for this reaction all the relevant information is available from various experiments. The experimental cross section could be reproduced assuming a direct mechanism and using the potential model and the folding procedure.

As a more general conclusion, we have confirmed for the ^{48}Ca region that the applicability of the statistical assumptions in the commonly used HF calculations to derive neutron–capture cross sections breaks down near magic shells. Rather, the cross section is dominated by one or a few resonances, or — as in our cases — by direct radiative capture to bound final states in the absence of low–lying CN resonances.

As we have shown, some experimental information on neutron–capture resonances — even far from stability — can be obtained from the decay model of β–delayed neutron emission. With regard to spectroscopic factors of bound states, they may be obtained from (d,p)–reactions in inverse kinematics using cooled radioactive beams.

ACKNOWLEDGEMENT

We are indebted to F.-K. Thielemann for making his code SMOKER available to us. We want to thank the Fonds zur Förderung wissenschaftlicher Forschung in Österreich (project S7307–AST) and the Österreichische Nationalbank (project 5054) for their support. TR acknowledges support by the Alexander von Humboldt foundation and by an APART fellowship of the Austrian Academy of Sciences.

---

[1] F. P. Cranston and D. H. White, Nucl. Phys. **A169**, 95 (1971).
[2] F. T. Seibel, E. G. Bilpuch and H. W. Newson, Ann. Phys. **69**, 451 (1972).
[3] W. D. Metz, W. D. Callender and C. K. Bockelmann, Phys. Rev. C **12**, 827 (1975).
[4] W. Ziegert, Diploma Thesis, Univ. Mainz (1980).
[5] L. C. Carraz et al., Phys. Lett. **109B**, 419 (1982).
[6] F. Käppeler, G. Walter and G. J. Mathews, Astrophys. J. **291**, 319 (1985).
[7] R. F. Carlton, J. A. Harvey, R. L. Macklin, C. H. Johnson and B. Castel, Nucl. Phys. **A465**, 274 (1987).
[8] V. F. Sears, Neutron News, **3**, 26 (1992).
[9] Y. Uozumi, O. Iwamoto, S. Widodo, A. Nohtomi, T. Sakae, M. Matoba, M. Nakano, T. Maki and N. Koori, Nucl. Phys. **A576**, 123 (1994).
[10] D. G. Sandler, S. E. Koonin and W. A. Fowler, Astrophys. J. **259**, 908 (1982).
[11] W. Hillebrandt, K.–L. Kratz, F.–K. Thielemann and W. Ziegert, in *Proceedings of the Int. Symp. on Weak and Electromagnetic Interaction in Nuclei, Heidelberg, Germany, 1986*, p. 987.
[12] K.–L. Kratz, W. Ziegert, W. Hillebrandt and F.–K. Thielemann, Astron. Astrophys. **125**, 381 (1983).
[13] M. Divadeenam, W. P. Beres and H. W. Newson, Ann. Phys. **69**, 428 (1972).
[14] A. Dobado and A. Poves, in *Proceedings of the Summer School on Heavy Ion Collisions, La Rabida, Spain, 1982, Lecture Notes in Physics 168*, (Springer, Berlin, 1993),p. 248–255 and private communication.
[15] P. Möller and J. Randrup, Nucl. Phys. **A541**, 1 (1990).
[16] J. J. Cowan, F.–K. Thielemann and J. W. Truran, Physics Report **208**, 267 (1991).
[17] Ch. Zhou, Nucl. Data Sheets **63**, 229 (1991).
[18] G. Audi and A. H. Wapstra, Nucl. Phys. **A565**, 1 (1993).
[19] J. Krumlinde and P. Möller, Nucl. Phys. **A417**, 419 (1984).
[20] H. Oberhummer and G. Staudt, in *Nuclei in the Cosmos*, edited by H. Oberhummer, (Springer, Berlin, 1991), p. 29–59.
[21] K. H. Kim, M. H. Park and B. T. Kim, Phys. Rev. C **35**, 363 (1987).
[22] B. G. Bailey, G. M. Griffiths and T. W. Donnely, Nucl. Phys. **A94**, 502 (1967).
[23] H. de Vries, C. W. de Jager and C. de Vries, At. Data Nucl. Data Tables **36**, 495 (1987).
[24] A. M. Kobos, B. A. Brown, R. Lindsay and G. R. Satchler, Nucl. Phys. **A425**, 205 (1984).
[25] H. Krauss, Code TEDCA, unpublished.
[26] A. Hauser, Code VOLD, unpublished.
[27] F.-K. Thielemann, private communication.

FIG. 1. Beta–delayed neutron spectrum of $J^\pi = 1/2^+$ ^{51}K decay.

FIG. 2. Contributions to the direct–capture cross section at 30 keV projectile energy as a function of the radial distance from the target nucleus.

FIG. 3. Comparison of the calculated direct–capture cross section (solid line) with the experimental data of ^{48}Ca(n,γ)^{49}Ca for projectile energies from the meV to the MeV region [1],[6],[7].

TABLE I. Spins, excitation energies, Q–values and spectroscopic factors of levels in ^{49}Ca [9].

J^π	$E_{\rm ex}$ [MeV]	Q [MeV]	S
$2p_{3/2}$	0.000	5.142	0.84
$2p_{1/2}$	2.021	3.121	0.91
$1f_{5/2}$	3.586	1.556	0.11
$2f_{5/2}$	3.993	1.149	0.84
$3p_{3/2}$	4.069	1.073	0.13
$3p_{1/2}$	4.261	0.881	0.12

TABLE II. Maxwellian–averaged direct–capture cross sections for neutron capture in ^{48}Ca.

J^π	$\langle\sigma(25\,\mathrm{keV})\rangle$ [mb]	$\langle\sigma(30\,\mathrm{keV})\rangle$ [mb]
$2p_{3/2}$	0.872	0.791
$2p_{1/2}$	0.244	0.222
$1f_{5/2}$	0.000	0.000
$2f_{5/2}$	0.000	0.000
$3p_{3/2}$	0.022	0.020
$3p_{1/2}$	0.007	0.006
Sum	1.145	1.039

TABLE III. Theoretical and experimental cross section for the capture reaction ^{48}Ca(n,γ)^{49}Ca.

ENERGY[a]	REFERENCE OF EXPERIMENTAL DATA	EXPERIMENTAL CROSS SECTION	DIRECT CAPTURE CROSS SECTION
0.0253 eV (M. a.)	Cranston and White [1]	(1.09 ± 0.14) b	1.13 b
25 keV (M. a.)	Käppeler et al. [6]	(1.03 ± 0.09) mb	1.15 mb
30 keV (M. a.)	Carlton et al. [7]	(1.05 ± 0.13) mb	1.04 mb
97 keV	Käppeler et al. [6]	(0.55 ± 0.09) mb	0.58 mb

[a]M. a. Maxwellian averaged.

TABLE IV. Spins, excitation energies, Q–values and spectroscopic factors of levels in ^{51}Ca [15].

J^π	$E_{\rm ex}$ [MeV]	Q [MeV]	S
$2p_{3/2}$	0.000	4.400	0.80
$2p_{1/2}$	1.177	3.223	0.92

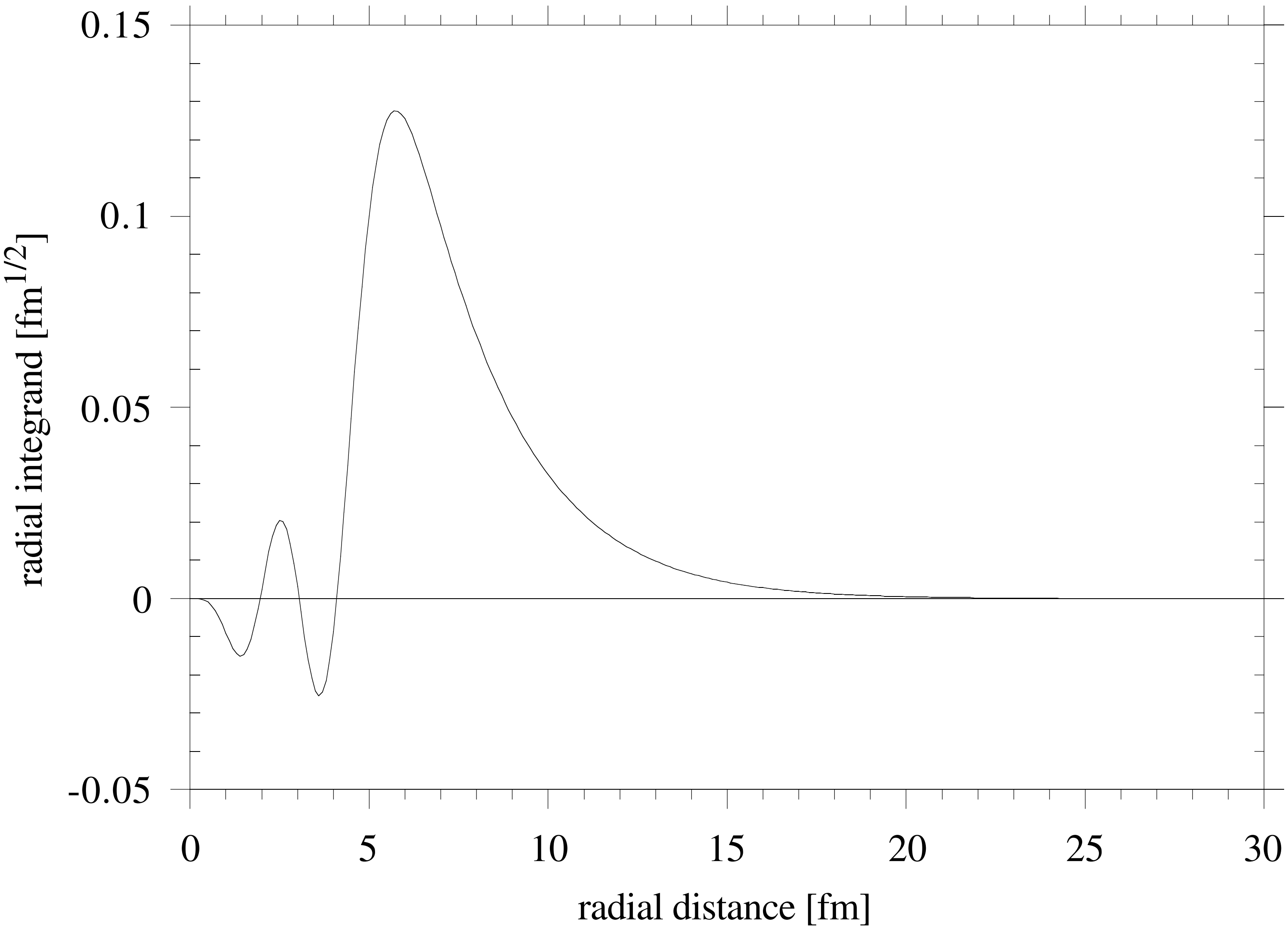

0.15
0.1
0.05
0
-0.05
radial integrand [fm^1/2]
0
5
10
15
20
25
30
radial distance [fm]

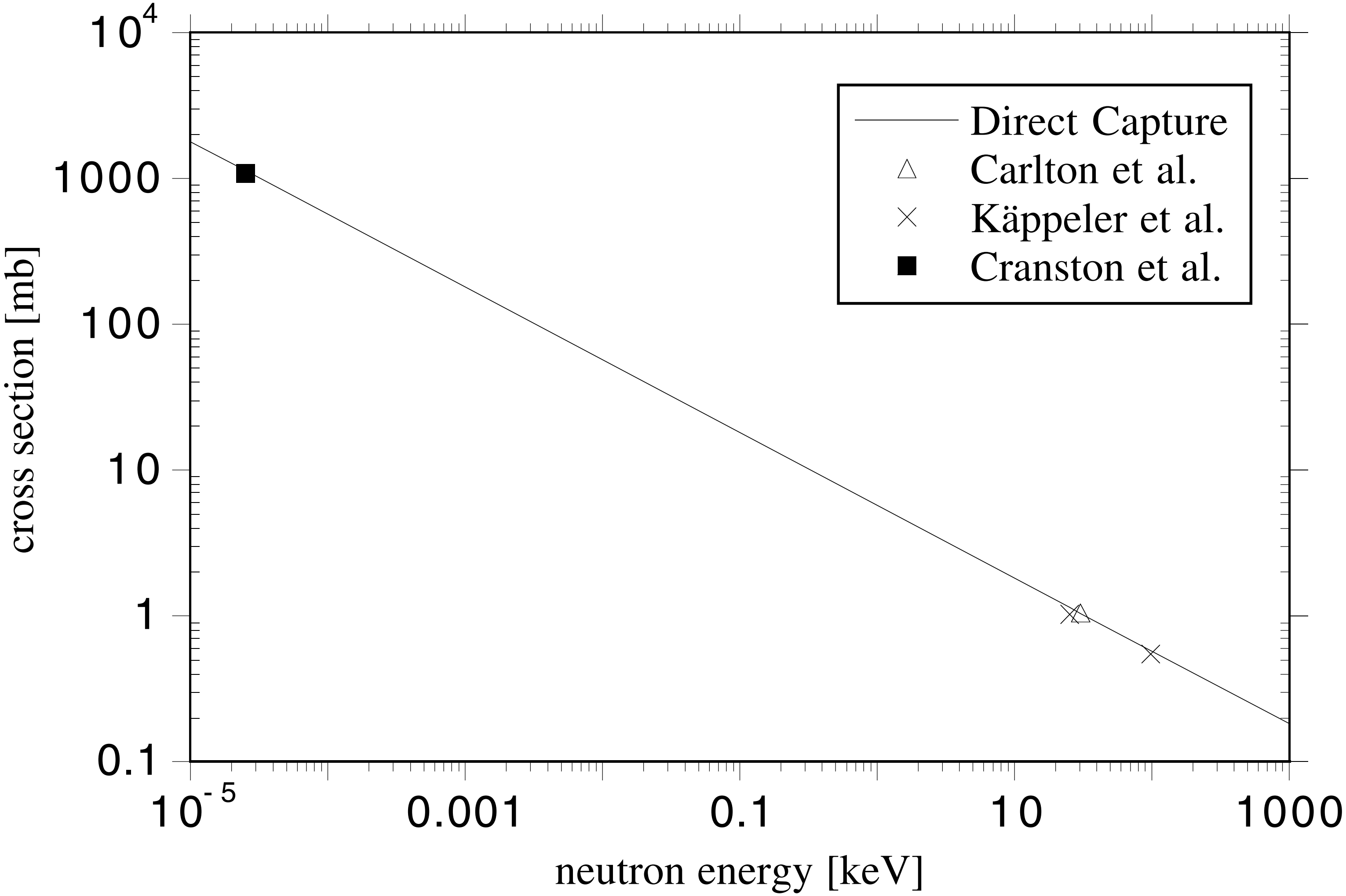

Direct Capture
Carlton et al.
Käppeler et al.
Cranston et al.
cross section [mb]
10^4
1000
100
10
1
0.1
10^-5
0.001
0.1
10
1000
neutron energy [keV]